Time-delay distribution as a probe of topological charge.

Marijn Man

Supervisors: Mikhail Titov and Piet Brouwer
Second corrector: Stephan Wiedmann

Bachelorthesis
Radboud University

June 28, 2015

Contents

1 Introduction and background information

In this thesis we are going to study the Wigner time-delays in quantum dots and in particular the difference in the time delay distribution between different topological subclasses for nonperfect coupling, corresponding to a different charge. Quantum dots are quantum wells in a semiconductor, which are small in all three dimensions [10]. Because the dots are so small they are distribed by quantum mechanics. They are also chaotic. This is the quantum mechanical analogue of classical chaos, which sates that the path of particles moving through the system is unpredictable. In order to study the behaviour of electrons moving through the dot we imagine we add a lead (or several leads) to the system and let electrons move through this lead, with one lead we are studying reflection. Electrons can enter or leave the system through different channels, which are states an electron can have while moving through the lead. A system with two leads with each one channel is the same as a system with one lead and two channels. When we describe the transport properties of the system we can use the scattering matrix S, S_{ij} gives the probability that an electron enters the system through channel i and leaves through channel j. The Wigner time delays we are studying are a way of measuring the time an electron entering the system remains in the system before it leaves, but this form of time delay (there are different ways to measure the time delay) is not really used for this purpose. Instead it is used in order to calculate the AC properties of current moving though the quantum dot. Our approach to studying these properties will be random matrix theory. This means in our case that we will describe the system by an Hamiltonian of finite size with random elements. We will convert this Hamiltonian to a scattering matrix and calculate the time delays for this system. There are 10 classes of random matrices which are often studied in this situation of which 3 where known for a long time, since around 1950 [6], and 7 are more recent, discovered around 2000 [1]. In this thesis we will study one of the classes which is known for a long time (class A), mostly for verification and comparison, and one class which is more recent (class D). The distribution of the time delays for both of these cases is already known, but we are going to extend these results to the case of nonperfect coupling. This means that we no longer assume that every electron trying to enter the system through the lead will actually enter the system, instead there is a certain probability that the electron will be reflected before it can enter the system. Because this calculation can become very complex very quickly if the number of channels increases we will only calculate the analytic result for class A with one channel and part of the calculation class D with two channels (but this last calculation can easily be generalised to a larger number of channels). We will also numerically calculate the time-delay distribution for other cases.

2 Random matrix theory (RMT)

2.1 The Gaussian ensemble

In random matrix theory a (quantum-)system is described by a finite dimensional matrix H with random elements, in our case this matrix represents the Hamiltonian of the system. Systems that can be described by random matrix theory are systems which are chaotic. Often a matrix is chosen with the following probability distribution [2]:

$$P(H) \propto e^{\frac{-c}{N}\mathrm{Tr}(H^2)} = \prod_{i,j} e^{-\frac{c}{N}H_{i,j}^2}$$

In with c a number which depends on N, N the dimension of the matrix H and $H = H^\dagger$. Often c is chosen in such a way that the eigenvalues of H in the limit of $N \to \infty$ range from -2 to 2, as described below. The second half of this formula shows that each element of the matrix is independently normal distributed. Therefore the distribution is called the Gaussian ensemble.

2.1.1 The energy levels and the Wigner semicircle

In random matrix theory we try to study the probability distributions of properties of matrices, when the matrices are chosen at random from ensembles. Often these probability distributions don't depend on the specific probability distribution used for A_{ij} (where A is the matrix). An example of such a property is formed by the eigenvalues of the Hamiltonian, which represent the energy levels of the system. For many different choices for the matrix distribution the eigenvalues of the system are distributed according to the Wigner semicircle (but this is not correct for all the symmetryclasses described below. In Fig. 1 the eigenvalues of the Hamiltonian are show for the Gaussian distribution ($H = H^\dagger$, class A).

2.2 Symmetry and topological classes in RMT

In order to describe different types of dots and environments we add symmetries to the Hamiltonian. So we add more constrains to the matrix H in addition to $H = H^\dagger$. In this way we can describe different types of systems or environments. If we add different combinations of the constraints from these symmetries we can get 10 different symmetry classes. 3 of which where known around the time the field first developed (class A, AI and AII). The other classes where added in the 90' by o.a. Altland and Zirnbauer. The different classes and some properties of these classes are described in the paragraphs below.
Some of these classes can be split up according to the topological class in which the system resides. The topology splits a class of insulators into several subclasses. Some classes can't be split up by topology, other classes such as D have two distinct topological subclasses and some classes have an infinite number of distinct subclasses.

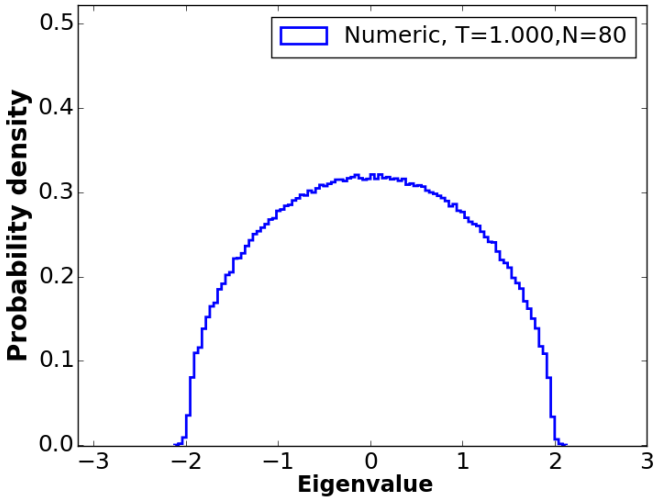

Figure 1: The distribution of the eigenvalues of a 80x80 random matrix, with each element distributed according to the Gaussian distribution. This distribution converges to the Wigner semicircle as the dimention of the matrix tends to infinity.

Below we list the different symmetries followed by the classes we will consider in this thesis:

2.2.1 Time reversal symmetry (TRS)

Time reversal symmetry has two different types TRS+1 and TRS-1 [9]. H must satisfy the following equation:

$$H = CH^T C^{-1}$$

, with $CC^\dagger = 1$ and $C = \pm C^T$, for TRS+1 (up) and TRS-1 (down) [9]. The derivation for this result can be found in [9]. We can choose $C = I$ for TRS+1 and σ_y for TRS-1 [9], in which σ_y is the Pauli spinmatrix.

2.2.2 Particle hole symmetry (PHS)

Particle hole symmetry also has two different types PHS+1 and PHS-1 [9]. H must satisfy the following equation:

$$H = -DH^T D^{-1}$$

, with $DD^\dagger = 1$ and $D = \pm D^T$, for PHS+1 (up) and PHS-1 (down) [9]. the derivation can again be found in [9]. We for PHS+1 can choose $D = \sigma_x$ [9], but

we can also choose $D = I$ [8], the last option is called the Majorana basis states that H is an imaginary matrix [8]. For PHS-1 we can chose $D = \sigma_y$ [9]. This symmetry senses the presence of a superconductor [3].

2.2.3 Chiral Symmetry (CS)

The last symmetry is a combination of the previous two. If we apply both TRS and PHS the system satisfies CS [9]. So H mus satisfy the following equation:

$$H = -UHU^{-1}$$

, with $UU^{\dagger} = 1$ and $UU = 1$ [9]. We can choose $U = \sigma_z$ [9].

2.2.4 The classes used in this thesis (A and D)

In this thesis we will use the classes A and D, therefore we will describe these two classes here. For a description of the other classes we refer to [9] (that thesis does not describe different topological subclasses, for which other references such as [3] should be consulted). Class A is the simplest class and does not have additional symmetries. So a matrix from class A is just a general hermitian matrix. Class D is a matrix with only PHS+1, this gives a hermitian imaginary matrix in the Majorana basis or $H = -\sigma_x H^T \sigma_x$ in the default choice. Class D has two topological classes. A matrix H from Class D is topological trivial if the dimension of H is even and topological nontrivial if the dimension of H is odd. The systems in the nontrivial subclass have a Majorana Fermion at $E = 0$, while the systems in the trivial subclass do not have such a particle [3]. Because we can only create both even and odd matrices in the Majorana basis we can only study the topological subclasses in this basis.

2.3 The scattering matrix

If we want to study the scattering of electrons from a system we have to calculate the scattering matrix (S). This matrix must have a much smaller dimension than H. The columns (and rows) of the scattering matrix each represent a different channel of the matrix and S_{ij} gives the probability that and electron entering the dot through channel i leaves the dot through channel j. We call the dimension of H N and the dimension of S M. So $i, j \in \{1, ...M\}$, with $M \ll N$ and M is equal to the number of channels. The S-matrix is not hermitian such as the Hamiltonian described above, instead it it unitary ($SS^{\dagger} = 1$). We can calculate this matrix with the the following formula [2]:

$$S = 1 - 2\pi i W^{\dagger}(E - H + i\pi W W^{\dagger})^{-1} W \tag{1}$$

E is the energy at which we are looking. In this thesis we will always assume that E=0, because most of the interesting phenomena take place at this energy. The matrix W describes the coupling of the dot and the lead. Because there are less channels than energy levels, the matrix W will be rectangular. W can

be chosen rectangular diagonal and diagonal elements are then given by the following formula [2]:

$$w_i = \sqrt{\frac{M\delta}{\pi^2 T_i}(2 - T_i \pm \sqrt{1 - T_i})}$$

In this formula T_i is the probability of an electron moving from the i^{th} channel into the system without being reflected and $i \in \{1, ..., M\}$. We can alternatively look at the matrix $W^\dagger W$, which is a square MxM matrix. This matrix than has as nonzero eigenvalues $\{w_i^2\}$. Because the base of W is irrelevant this is enough to specify W for our purpose. Often $T = 1$ is assumed in which case we speak of perfect coupling. In this thesis we will also look at the case $T \neq 1$. Here δ is the mean level spacing, which is the mean distance between adjacent unique energy levels in the bulk of the energy level distribution. In class D all the physical scattering matrices have an even dimension, the reason for this is that for each channel consisting of electrons there must be a corresponding channel for the holes [3]. In class A there is no such restriction.

2.3.1 The circular ensemble

If E=0 we can also study the scattering matrix directly, without the Hamiltonian. In the case of perfect coupling the scattering matrix is given by the circular ensemble. If we create a matrix according to the circular ensemble we assume that the probability density is constant for each matrix [2]. In the case of just one channel in class A this corresponds to $S = e^{i\phi}$, with ϕ uniformly distributed over $[0, 2\pi]$. Unfortunately this matrix is energy independent and can therefore not be used to calculate the derative of S by E. This also means that the circular ensemble cannot be used to calculate time delays as we will see below.

2.3.2 From perfect to nonperfect coupling

In our analytic calculation of the time delays for nonperfect coupling we need a direct relation between the scattering matrix for perfect coupling (S_0) and the scattering matrix for nonperfect coupling (S). For this we can use the following formulas by [4]:

$$S = r + t' S_0 (1 - r' S_o)^{-1} t \tag{2}$$

In which r and t are diagonal matrices with elements $t_i = \sqrt{T_i}$ and $r_i = \sqrt{1 - T_i}$. We will assume that the probability of an electron being reflected by the barrier is equal for both sides of the barrier, this gives $r = -r'$, $t = t'$. According to Brouwer, this formula can be derived in the following way:
Assume we have an electron which has the wave function ψ and moves through the system. We want to determine the function ψ', which is the outgoing wavefunction. In order to do this we have to sum the probability times the original wavevector over all the different paths the electron can take to get there. First of all the electron can be immediately reflected, which gives a contribution of

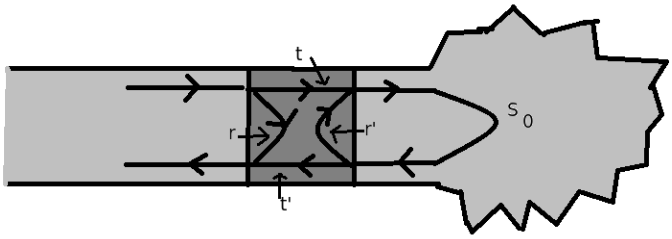

Figure 2: Sketch of a selection of the first few steps of the possible paths an electron can take when moving through a quantum dot with a tunnel barrier. If we extend paths from the yellow arrow at a similar fashion we can get all the possible paths, like we did in the derivation of formula 2.

r. Than there is a probability that the electron enters the system (this gives t), bounces n times against the barrier when it tries to return through the lead (multiply by $(r'S_0)^n$), and goes back into the system one last time (S_0) and than finally leaves the system (t). Adding all this together gives:

$$S = r + tS_0 \sum_{n=0}^{\infty} (r'S_0)^n t = r + tS_0(1 - r'S_0)^{-1} \tag{3}$$

2.4 Time delays

The time delays of the system are described by the eigenvalues of the time-delay matrix (Q), which is given by [8]:

$$Q = -i\hbar S^\dagger \frac{dS}{dE} \tag{4}$$

In a number of different articles the distributions for these eigenvalues are calculated for different symmetry classes, we will list the results for class A and class D [8]. The results are in terms of $\gamma = \tau^{-1}$. For class A [5]:

$$P(\{\gamma_s\}) \propto \prod_{i<j} |\gamma_i - \gamma_j|^2 \prod_s \gamma_s^N \exp(-\frac{2\pi\hbar\gamma_s}{\delta_0}) \tag{5}$$

Where δ_0 is the mean level spacing as described in previous sections and N is the dimention of S. And for class D [8]:

$$P(\{\gamma_i\}) \propto \prod_{i<j} |\gamma_i - \gamma_j| \prod_s \gamma_s^{-1+N/2} \exp(-\frac{1}{2}\frac{2\pi\hbar}{\delta_0}\gamma_k) \tag{6}$$

3 Numerically calculating the distribution of the time delays

In this thesis we will calculate the probability distribution of time delays for the classes A and D, with both perfect and nonperfect coupling. The actual goal is to compare the time-delay distribution for the nontrivial subclass of class D with the results for the topological trivial subclass of class D and see if there is any difference. We will use the results for class A (and 1 channel) in order to test the working of our program, by comparing it to the analytic results for this case.

3.1 The program

Our program calculates the probability distribution of the time delays (and several other properties of H and S) by creating a large number of Gaussian matrices, for instance 100,000 matrices, (which represent the Hamiltonians). Later we use fromula (1) in order to get the corresponding scattering matrices. Finally we will obtain the time-delay matrix, with equation (4) and calculate the eigenvalues. By collecting the time delays of a large number of random systems we get a distribution for the time delays. We use scipy (a scientific package for python [7]) and will use multiprocessing in order to use all cores of the CPU, which will make our program faster.

3.1.1 Generating the matrices

There are two ways to generate the random matrices of the different symmetry classes. First we will outline a general method, followed by the method we actually used in our program. Assuming we have a symmetry of the form (7):

$$H = Sf(H)S^{-1} \tag{7}$$

We can first generate a Hamiltonian without the symmetry (H') and than use:

$$H = \frac{1}{2}(H' + Sf(H')S^{-}1)$$

This makes sure that:

$$Sf(H)S^{-1} = \pm Sf(0.5(H' \pm Sf(H')S))S = H$$

If f is the hermitian conjugate, the transpose or the identity operator and S has the property $SS^T = \pm 1$. So that the symmetry is satisfied. Although this takes care of the symmetry it also removes the normalisation of the Hamiltonian such that the eigenvalues no longer range from -2 to 2, because H' and $Sf(H')S$ can partially cancel each other out. So the normalisation must be resort by multiplying H by a constant. The other way is by looking at the matrices in more detail and making sure that the matrix is in the required form. In our program we chose for the second option. For the classes A and D this required form is rather simple, as described in previous sections we get: $H = H^\dagger$ for class A and $H = iA$, with A a real matrix, for class D in the Majorana basis.

3.2 Validation of the program

3.2.1 Validating the symmetries

For class A and the Majorana basis for class D this isn't that important, because the symmetries are very simple. If we would use more complex symmetry classes we could validate that our matrices satisfy the requirements by explicitly testing them on 8x8 matrices.

3.2.2 Validating the formula for S (and Q)

We have validated the formula for S in a number of different ways. First we have checked that the probability distribution for the angles of the eigenvalues for S is (almost) uniform in the A symmetry class. When this was the case we went to checking the distribution of the eigenvalues for Q, which we also did for class A. First we used the probability distribution function for the eigenvalues of Q, with perfect coupling, from 6 in the case of just one channel. Then we used the derived formula (15) for the probability distribution for nonperfect coupling in the case T=0.5 (and one channel) and made sure the analytic distribution gave the same result as the numeric answer. The results are displayed in in Fig. 3:

3.3 The time-delay distributions for different topological subclasses

We plotted the probability distribution function for the time delays for both topological classes of class D, we used H of dimension 80, 81 and for some calculations 160 and 161. We did this for T=1 for two channels, see Fig. 3.3, and found that there is indeed no difference in the probability distribution as [8] predicted.

3.3.1 A difference in the time-delay distributions for nonperfect coupling

We also plotted the probability distribution for T=0.5, see Fig. 3.3.1, and T=0.95, see Fig. 3.3.1, for two channels and found that the probability distribution of the two topological subclasses was different in these cases. Although the difference was smaller in the case of T=0.95, than in the case of T=0.5.

3.3.2 The effect of increasing the number of channels

We also made a plot of the probability distribution for T=0.5 with four channels instead of two to find out if the effect stays the same, if we increase the number of channels Fig. 3.3.2. Because we found that the size of the effect was diminished we also made a plot with 12 channels and T=0.5, in this case we saw that the difference between the two classes disappeared when we look at all the time delays, see Fig. 3.3.2. But when we looked at the distribution of only the largest time delay, we still found a difference, although this difference is smaller

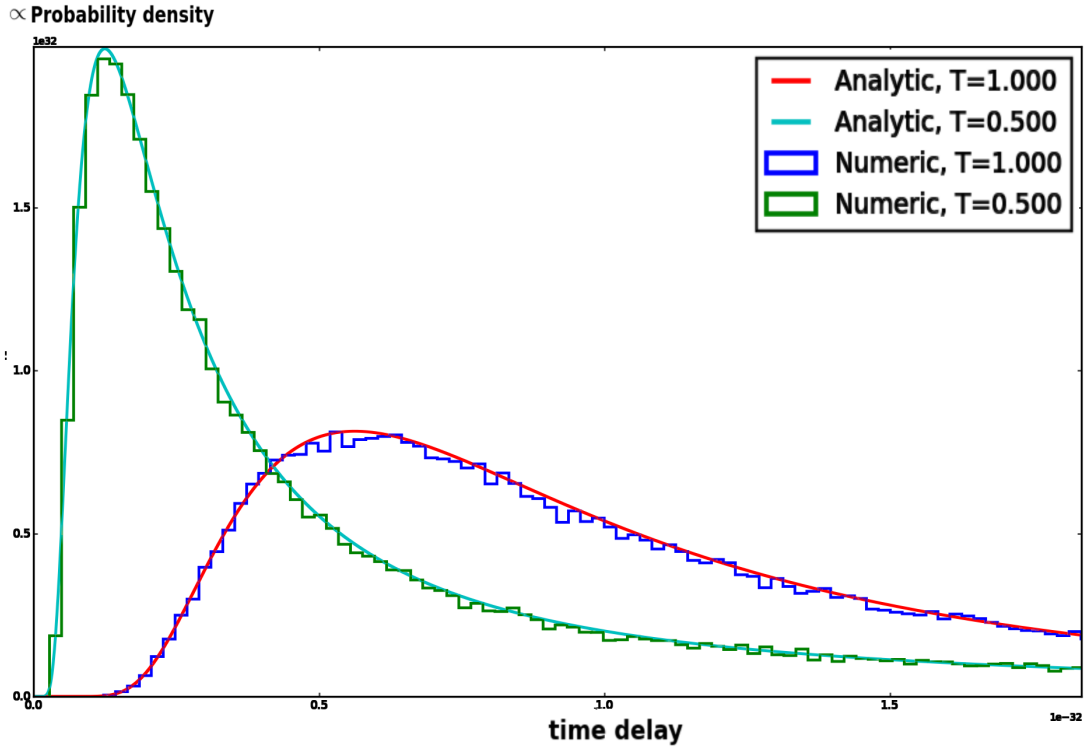

Figure 3: The probability distribution of the time delays in class A for T=1.0 and T=0.5. For both analytic and numeric results, we get the same distribution. As can be seen our analytic results agree nicely with our numeric results.

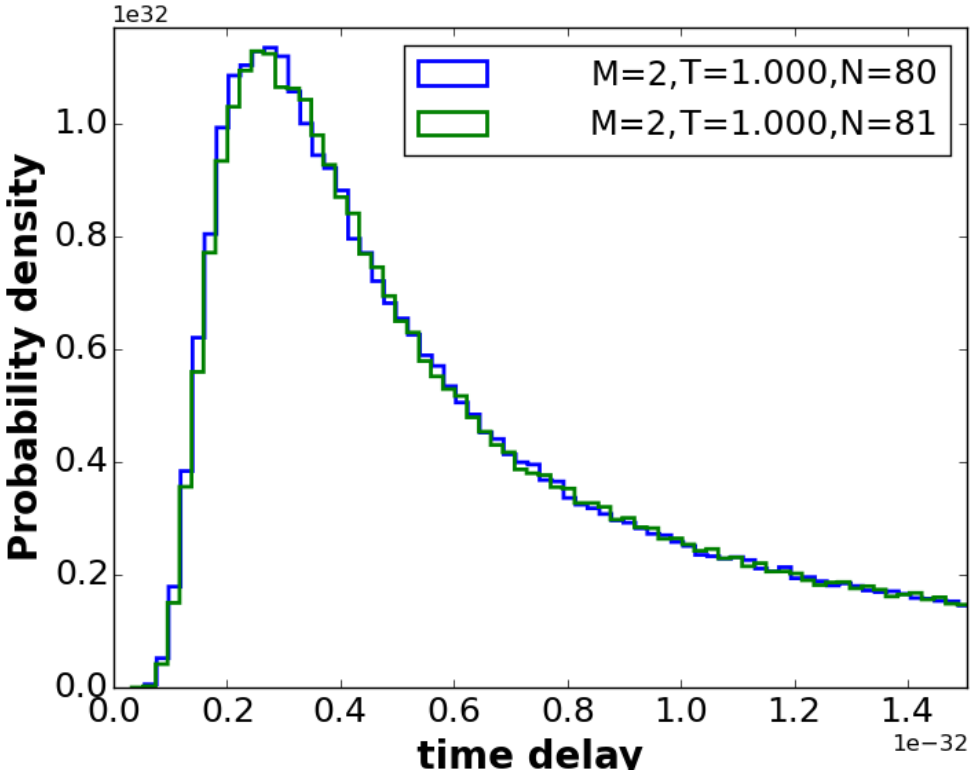

Figure 4: Plot of the probability distribution for the time delays in the two different topological subclasses of class D for perfect coupling and two channels. The system is topological trivial if $\dim(H)$ is even and otherwise topological nontrivial. The distribution of both cases are identical. In these plots M indicates the number of channels and N indicates the dimension of H.

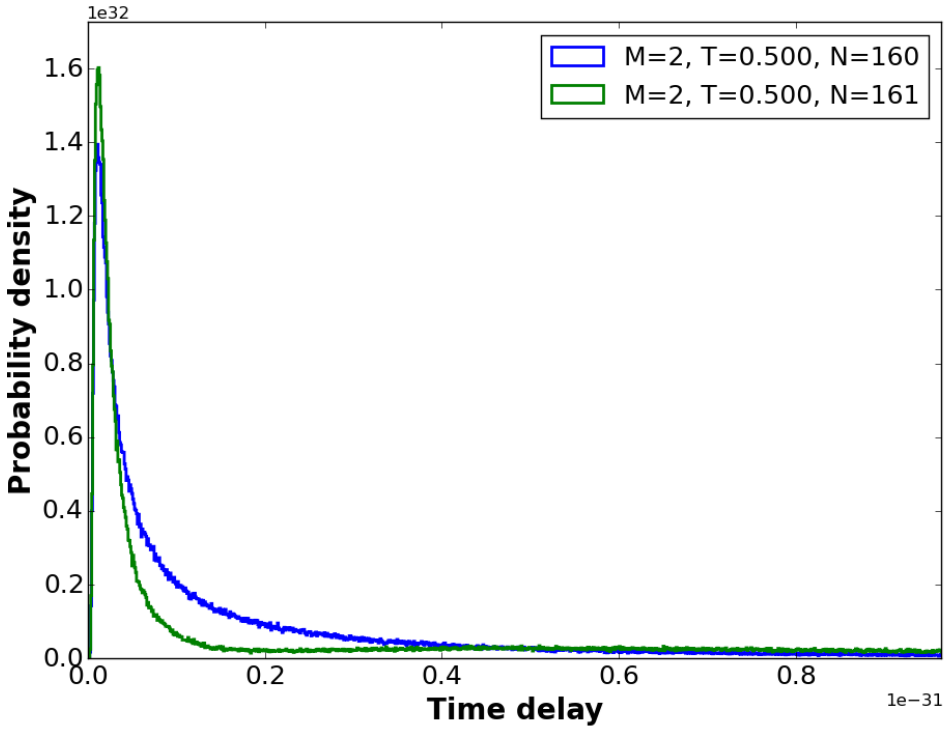

Figure 5: Plot of the probability distribution for the time delays in the two different topological subclasses of class D for T=0.5, with two channels. It can be seen that the distributions differ.

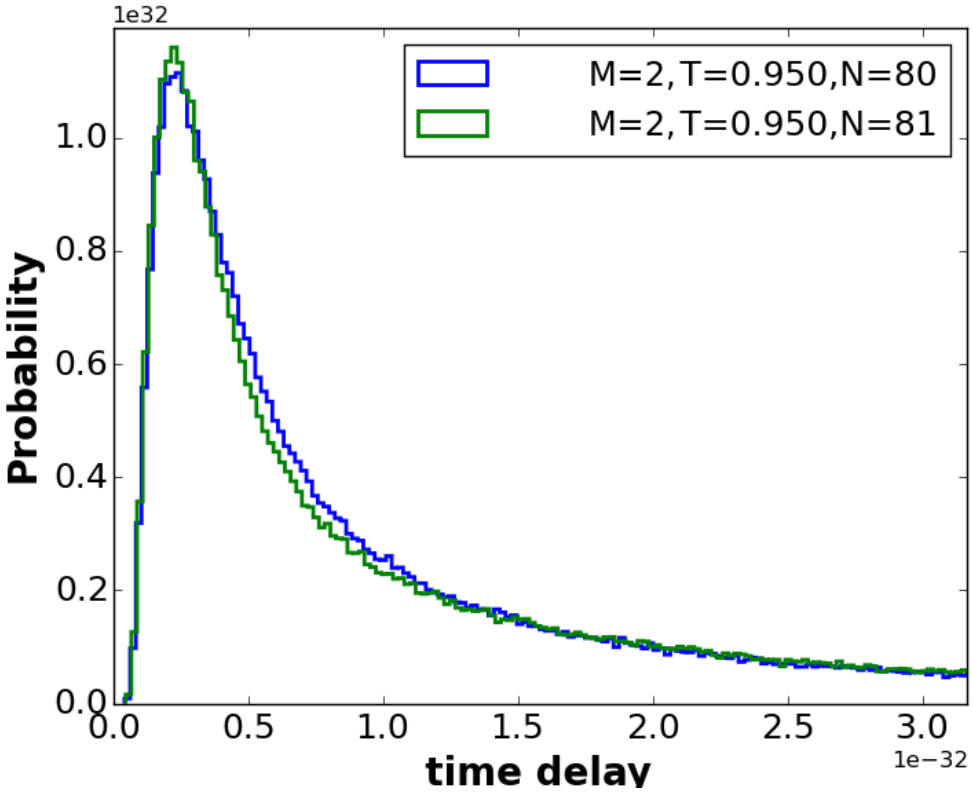

Figure 6: Plot of the probability distribution for the time delays in the two different topological subclasses of class D for T=0.95 and two channels, it can be seen that the distributions slightly differ.

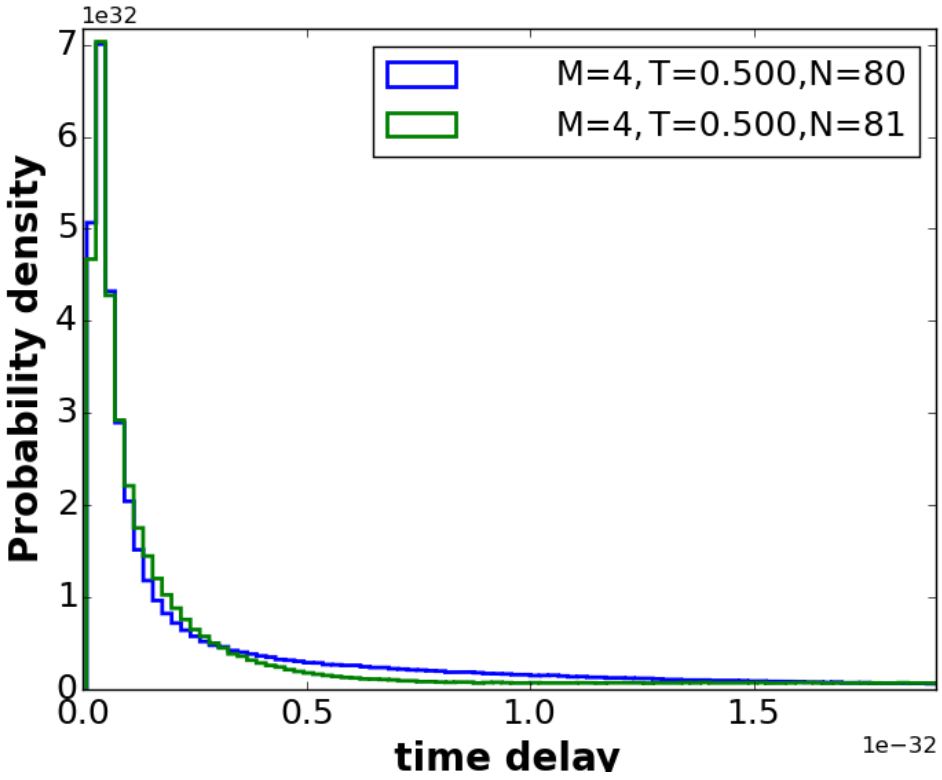

Figure 7: Probability distribution for the time delays in the two different subclasses of class D for T=0.5, with four channels.

and different than the original difference, see Fig. 3.3.2. We also looked at the smallest time delay, but in this case there was no difference between the distributions. In order to determine whether this effect was just because difference in the distribution of the largest time delay disappeared slower than the difference in the distribution of all the time delays we plotted the distribution for 20 channels. The result can be found in 3.3.2, it can be seen that the difference between the distributions of the largest time delay also becomes smaller.

4 Analytical computation of the time delays for nonperfect coupling

In this section we will calculate the time delays in an analytic way for class A, we will also start a more general calculation for class D (it would also work for

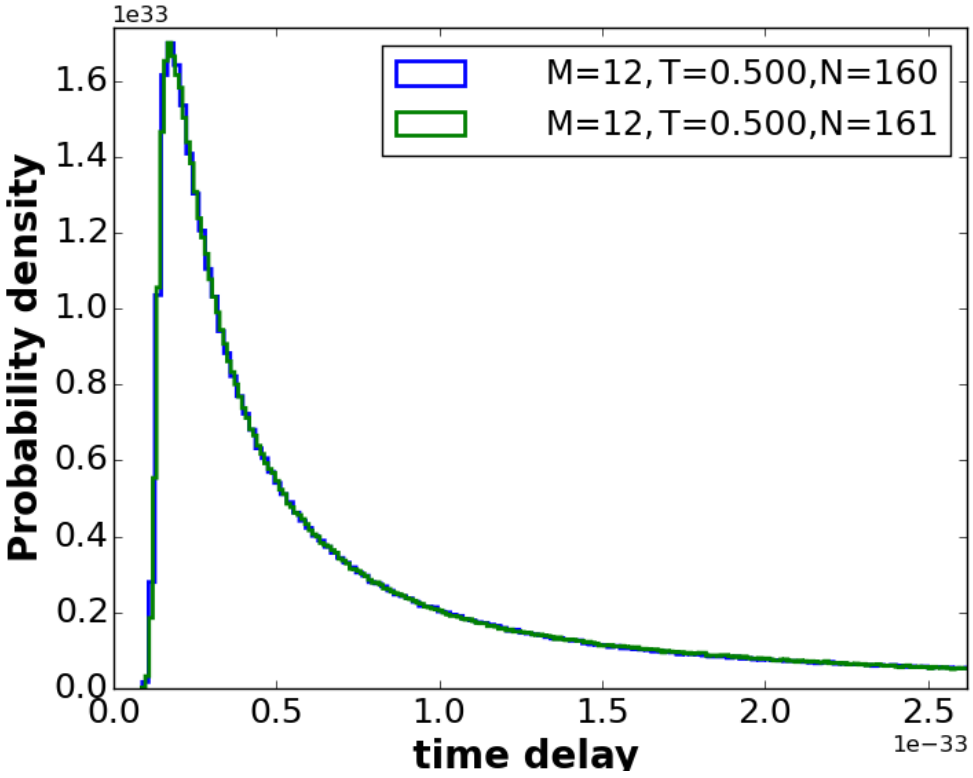

Figure 8: Probability distribution for the time delays in the two different subclasses of class D for T=0.5, with 12 channels. This plot suggests that the difference between the probability distributions for the two subclasses disappears if the number of channels increases.

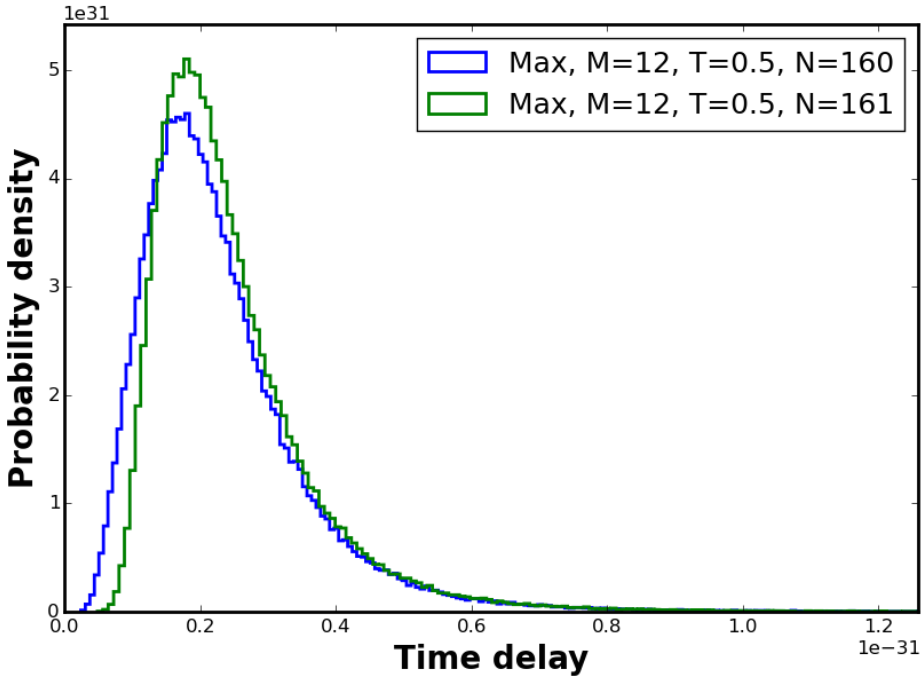

Figure 9: Probability distribution of the largest time delay in the system for the two different subclasses of class D for T=0.5, with 12 channels. This graph shows that the difference between the two classes is still apparent if we only look at the largest time delay.

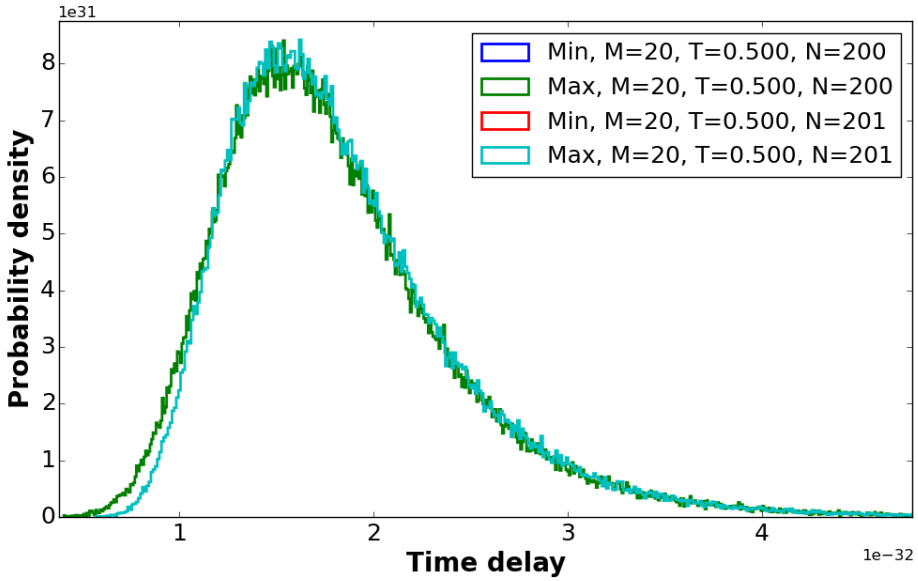

Figure 10: Probability distribution of the largest time delay in the system for the two different subclasses of class D for T=0.5, with 20 channels. This graph shows that the difference between the two classes also becomes smaller if we only look at the largest time delay.

similar classes). We will calculate the relation between Q and Q_0. In order to calculate the Jacobian and the actual distribution we first have to parametrise the equation, we will do this for class D with two channels, after this is done we get a rather complex system of equations. This system can be solved with the help of a program such as mathematica. Because the relation between Q and Q_0 and thus the resulting probability distribution is rather complex and therefore less useful we will not actually carry out this calculation, we also won't look at the parametrisation for more than two channels.

4.1 General principle behind the calculation

When we want to calculate the probability distribution in the case of nonperfect coupling we first have to parametrise the matrices involved (S in $\{\theta^{(i)}\}, Q$ in $\{\tau^{(i)}\}, S_0$ in $\{\theta_0^{(i)}\}$ and Q_0 in $\{\tau_0^{(i)})\}$, where S_0 and Q_0 are the matrices in the case of perfect coupling and the other two matrices are the nonperfect coupling versions of these matrices. Parametrising means writing a matrix in terms of a set of scalars, although we can select all the individual components of the matrix (or the real and imaginary part of a component in the complex case) as parameters we can often get a simpler parametrisation. We do this by making use of the constraints on the matrix. When this is done we calculate the parameters of S and Q in terms of the parameters of the perfect coupling matrices, using the formulas 2 and (4). When this is done we calculate the Jacobians for the transformation: $\frac{d\{\theta_0^{(i)}\}}{d\{\tau^{(i)}\}}$. Now we need to know the probability distribution of the time delays in the case of perfect coupling, which is listed in one of the previous sections. If we know all this information we can get the distribution in the case of nonperfect coupling by using the following formula:

$$P(Q, S_0) = P(Q_0(Q), S_0)\frac{d\{\theta_0^{(i)}\}}{d\{\tau^{(i)}\}}$$

Now we need to integrate over all the values of S_0. This can be done by means of the parametrisation of S_0. If analytic integration fails we can express the result in the form of an integral, which we can later numerically integrate. We can also look if there are limiting cases which can be integrated in an analytic way.

4.2 Calculation for class A with one channel

We can parametrise the matrices in the following way:

$$S_0 = e^{i\phi}, S = e^{i\theta}, Q_0 = \tau_0 \text{ and } Q = \tau \tag{8}$$

We also take $r = \sqrt{1-T}$ and $t = \sqrt{T}$, as defined before. Because we have only one channel these variables are now scalars. By using (4) and (8) we get:

$$\tau = -i\hbar e^{-i\theta}\frac{de^{i\theta}}{dE} \tag{9}$$

Now we can combine (2) and (8) to get:

$$e^{i\tau} = r + \frac{e^{-i\phi}}{1 + re^{i\phi}} \tag{10}$$

And now we can combine these two equations to get:

$$\tau = -i\hbar \left(r + \frac{e^{-i\phi}}{1 + re^{-i\phi}} \right) \frac{Tie^{i\phi} \frac{d\phi}{dE}(1 + re^{i\phi}) - re^{i\phi} i \frac{d\phi}{dE} Te^{i\phi}}{(1 + re^{i\phi})^2} \tag{11}$$

We have with equation (9), but now for perfect coupling:

$$\hbar \frac{d\phi}{dE} = \tau_0$$

Substituting this in (11) gives:

$$\tau = \frac{\tau_0 T}{2(1 + r\cos\phi) - T} \tag{12}$$

and

$$\frac{d\tau_0}{d\tau} = T^{-1}(2(1 + \cos\phi) - T) \tag{13}$$

Combining this with the time delays form 5 we get:

$$P_\tau(\tau; \phi) \propto \frac{\tau^{-3} T^2 \exp\left[-\tau_H \tau^{-1} (\frac{T}{2(1+r\cos\phi)-T} \right]}{(2(1 + r\cos\phi) - T)^2} \tag{14}$$

and

$$P_\tau(\tau) \propto \int_0^{2\pi} \frac{\tau^{-3} T^2 \exp\left[-\tau_H \tau^{-1} (\frac{T}{2(1+r\cos\phi)-T}) \right]}{(2(1 + r\cos\phi) - T)^2} d\phi \tag{15}$$

We checked that numerically integrating formula (15) gave the same result as our numerical calculation as described in 3.2.2. Note that we still use ϕ instead of θ in these formula's. Since we can't analytically calculate this integral we are also going to look at the Taylor expansion of this formula around r=0 and r=1: First we substitute $T = 1 - r$ and use the Series function from Mathematica [11] around r=0 and take the constant and linear term in the resulting Taylor expansion:

$$P_\tau(\tau; \phi) = -\frac{c \exp(-\frac{\tau_H}{\tau})}{\tau^3} + \frac{c \exp(-\frac{\tau_H}{\tau})(3\tau - 2\tau_H + 2(\tau - \tau_H)\cos\phi)}{\tau^4} r \tag{16}$$

Now we can integrate with respect to ϕ in order to obtain:

$$P_\tau(\tau) \approx \frac{2c \exp(-\frac{\tau_H}{\tau} \pi((-1 + 3r)\tau - 2r\tau_H)}{\tau^4} \tag{17}$$

In the case of r=1 we can't immediately use a Taylor expansion, instead we first have to change variables to $\tau' = \frac{\tau}{1-r}$, which gives:

$$P_\tau(\tau;\phi) \approx -\frac{c\exp\left[-\frac{\tau_H}{\tau'+r\tau'+2r\tau'\cos\phi}\right]}{(\tau')^3(1+r+2r\cos\phi)}$$

And the result of the Taylor expansion is now:

$$\begin{aligned} P_\tau(\tau) \approx & \frac{c(r-1)(2\cos\phi+1)\exp\left[-\frac{\tau_H}{\tau'(2\cos\phi+2)}\right](2\tau'\cos\phi+2\tau'-\tau_H)}{8\tau'^4(\cos\phi+1)^3} \\ & - \frac{c\exp\left[-\frac{\tau_H}{\tau'(2\cos\phi+2)}\right]}{\tau'^3(2\cos\phi+2)} \end{aligned} \tag{18}$$

Unfortunately we still cannot analytically integrate this formula.

4.3 Calculation for class D

4.3.1 General part

First we have to derive a formula for Q_0 in therms of Q, this can be done independent of the size and the class of the scattering matrix, as long as Q is given by formula (4). For some classes the distribution for the time delays is determined by examining another matrix Q' which has the same eigenvalues, this derivation will not necessary hold in that case. In this derivation we will assume that $t = \sqrt{T}$ and $r = \sqrt{1-T}$ are both multiples of the identity matrix. Inserting (2) in equation (4) we get:

$$Q = -i\hbar(r + tS_0(1+rS_0)^{-1}t)^\dagger \frac{d}{dE}(r + TS_0(1+rS_0)^{-1})$$

, so with $\frac{dA}{dt} = -A^{-1}\frac{dA}{dt}A^{-1}$ we get:

$$Q = -i\hbar(r+tS_0(1+rS_0)^{-1}t)^\dagger(T\frac{dS_0}{dE}(1+rS_0)^{-1} - TS_0(1+rS_0)^{-1}r\frac{dS_0}{dE}(1+rS_0)^{-1})$$

, substituting $\frac{dS_0}{dE} = (i\hbar)^{-1}S_0Q_0$ we get:

$$Q = T(r + T(1+S_0^\dagger r)^{-1}S_0^\dagger)(1 - S_0(1+rS_0)^{-1}r)S_0Q_0(1+rS_0)^{-1}$$

, this gives Q_0 in terms of Q:

$$Q_0 = (T(r + T(1+S_0^\dagger r)^{-1}S_0^\dagger)(1 - S_0(1+rS_0)^{-1}r)S_0)^{-1}Q(1+rS_0)$$

4.3.2 Parametrisation for two channels

We have to find a parametrisation for Q (calculation by Brouwer), we know that:

$$S = S^*$$

and S is unitary, because S is orthogonal [3]. Because of (4) we know that $Q = Q^\dagger$ and $Q = Q^*$ (we look at E=0). This means that Q is real and symmetric, so:

$$Q = \begin{pmatrix} \cos\phi & \sin\phi \\ -\sin(\phi) & \cos\phi \end{pmatrix} \begin{pmatrix} \tau_1 & 0 \\ 0 & \tau_2 \end{pmatrix} \begin{pmatrix} \cos\phi & -\sin\phi \\ \sin\phi & \cos\phi \end{pmatrix} \tag{19}$$

This equation gives a parametrisation for Q and Q_0. The other matrices we need to parametrise are S and S_0. Because S and S_0 are orthogonal, there are two possible parametrisations for these matrices:

$$S_{(0)} = \begin{pmatrix} \cos\theta_{(0)} & \sin\theta_{(0)} \\ -\sin\theta_{(0)} & \cos\theta_{(0)} \end{pmatrix} \tag{20}$$

Or:

$$S_{(0)} = \begin{pmatrix} \cos\theta_{(0)} & \sin\theta_{(0)} \\ \sin\theta_{(0)} & -\cos\theta_{(0)} \end{pmatrix} \tag{21}$$

Now that we have a parametrisation for the different matrices and a relation between Q and Q_0 we can calculate the probability distribution function with the help of a program such as Mathematica. But the result of such a calculation would be to complicated to represent in this thesis.

5 Conclusion

According to [8] the time delays of a class D system are independent of the topological subclass of the system. It is also stated that some spectral properties are distinct between topological classes in the case of tunnelled coupling, but this difference disappears in the case of perfect coupling. In this thesis we looked at the time-delay distribution 4 in the case of perfect and nonperfect coupling. We found that the search for an analytic formula for the time delays in the case of nonperfect coupling is infeasible, because of the large size of the resulting formulas as soon as the number of channels is larger than one. So we could not use analytic results to analyse the time delays. Instead we used numeric calculations. These numeric calculations showed that the time delays for the two different topological classes are different in the case of nonperfect coupling. Furthermore we found that this divergence already starts at values for T which are very close to the case of perfect coupling, although the difference is still very small as long as T is close to 1. But we only saw this effect in the distribution of all the time delays together for systems with a small number of channels and also saw this effect diminish if we look at the largest time delay. When we switched from two channels, which is the smallest number of channels which makes physically sense, to four channels we saw that the effect on the total distribution became smaller. We also looked at the difference in probability distribution for a system with a large number of channels (12) and saw that the difference between the two topological subclasses disappeared in the total distribution. When we only looked at the largest time delay of a given system instead of all the time delays we saw that the difference returned, although this

difference was less apparent. When we increased the number of channels to 20 we saw that the difference became smaller for the maximum time delay.
So we saw that the time-delay distribution for the two topological subclasses of class D differed in the case of nonperfect coupling. This effect diminished when the system approached perfect coupling. We also saw that the effect decreased when we increased the number of channels. When we look at all the channels together the effect disappeared quickly, but if we only looked at the largest time delay the effect was apparent for a larger number of channels. So we conjecture that the distribution of the maximum time delay of a system is more sensitive than the distribution of all the time delays taken together.

References

[1] Alexander Altland and Martin R. Zirnbauer. Nonstandard symmetry classes in mesoscopic normal-superconducting hybrid structures. *Phys. Rev. B*, 55:1142–1161, Jan 1997.

[2] C. W. J. Beenakker. Random-matrix theory of quantum transport. *Rev. Mod. Phys.*, 69:731–808, Jul 1997.

[3] C.W.J. Beenakker. Random-matrix theory of majorana fermions and topological superconductors. *arXiv*, 2014.

[4] P. W. Brouwer. Generalized circular ensemble of scattering matrices for a chaotic cavity with nonideal leads. *Phys. Rev. B*, 51:16878–16884, Jun 1995.

[5] P. W. Brouwer, K. M. Frahm, and C. W. J. Beenakker. Quantum mechanical time-delay matrix in chaotic scattering. *Phys. Rev. Lett.*, 78:4737–4740, Jun 1997.

[6] Thomas Guhr, Axel MllerGroeling, and Hans A. Weidenmller. Random-matrix theories in quantum physics: common concepts. *Physics Reports*, 299(46):189 – 425, 1998.

[7] Eric Jones, Travis Oliphant, Pearu Peterson, et al. SciPy: Open source scientific tools for Python, 2001–. [Online; accessed 2015-06-13].

[8] M. Marciani, P. W. Brouwer, and C. W. J. Beenakker. Time-delay matrix, midgap spectral peak, and thermopower of an andreev billiard. *Phys. Rev. B*, 90:045403, Jul 2014.

[9] R.M. Noest. Topological classification of insulators and superconductors. Master's thesis, uva, Jul 2010.

[10] MA REED, JN RANDALL, RJ AGGARWAL, RJ MATYI, TM MOORE, and AE WETSEL. OBSERVATION OF DISCRETE ELECTRONIC

STATES IN A ZERO-DIMENSIONAL SEMICONDUCTOR NANOSTRUCTURE. *PHYSICAL REVIEW LETTERS*, 60(6):535–537, FEB 8 1988.

[11] Inc. Wolfram Research. Mathematica 10.1.